

双稳态屈曲梁压电发电结构非线性动力学分析*

曹东兴[†] 孙培峰 姚明辉 胡文华 张伟

(北京工业大学机电学院 机械结构非线性振动与强度北京市重点实验室, 北京 100124)

摘要 建立了磁场力作用下双稳态屈曲梁发电结构非线性动力学方程,利用 Galerkin 离散和多尺度方法分别分析了一阶离散和二阶离散系统的非线性动力学特性. 分析了系统阻尼、外激励幅值和外激励频率对该发电结构振动特性的影响,获得了频率响应曲线;分析了系统在 1:2 内共振情况下动力学行为,数值结果表明系统存在倍周期运动和混动运动.

关键词 双稳态, 屈曲梁, 压电发电, 非线性动力学

DOI: 10.6052/1672-6553-2016-017

引言

双稳态结构多应用于微电子机构,其研究始于 90 年代,在 21 世纪初取得巨大进展. 现阶段研究的方向主要分两个,一是利用双稳态微结构自身两个稳态的特性制作微结构开关,另一方面利用双稳态结构响应带宽较大,结构简单耐用等特性制作能量收集装置. 本文将结合双稳态结构能够扩展系统响应带宽的特点设计一种双稳态屈曲梁压电发电结构并分析其非线性动力学特性.

屈曲梁是一种常见的双稳态结构,1997 年,季进臣^[1]固定一端滑动承受轴向简谐载荷的屈曲梁的非线性响应进行了实验. 研究了基本参数和共振两种情况,揭示了系统倍周期分岔和混沌等复杂动力学行为. 1998 年, Vangbo^[2]基于经典细长梁,同时考虑压力影响,给出了两边铰接梁稳态变化的理论建模方法. 1998 年,叶敏^[3]考虑一端具有干摩擦的弹性屈曲梁在轴向激励下的非线性振动系统,研究了系统中初始屈曲度、阻尼、频率、激励振幅等各种物理参数对 1/2 亚谐共振情况下倍周期分岔的影响. 2000 年, Saif^[4]提出了一个简化微机械结构双稳态系统. 模型阐释了梁轴向弹性缩短,以及梁和激振器之间非线性关系. 2007 年,赵剑^[5]基于广义变分原理,借助半纯函数公式解析地给出了预压屈曲梁双稳态跳跃过程中横向力与位移之间的

非线性关系式. 2007 年, Hiroshi Yabuno^[6]研究了屈曲梁在高频激励下的响应. 2009 年, Fernandes^[7]等对非中部激励的双稳态屈曲梁进行了建模与实验. 发现在非中部荷载情况下,双稳态转化过程会出现迟滞现象.

压电振动能量采集近年来引起国内外学者的广泛关注. 麻省理工学院的 Shenck 等^[8]研究了脚跟着地时的能量损失,将多层 PVDF 薄窄板安装在鞋底用于提取人在行走时鞋底变形产生的能量. Erturk 和 Inman^[9-10]深入研究了基于 Euler - Bernoulli 梁的悬臂式压电俘能器,推导出了力学响应、电压、电流以及输出功率的简单表达式. 杨增涛^[11]指出双压电晶片梁弯曲模式采集器用于吸收低频环境振动能,板或壳体厚度模式采集器用于吸收高频环境振动能,螺旋形俘能器和波纹板俘能器也可用于低频情况. 2010 年, Ravindra^[12]对轴向荷载下的双稳态俘能器进行了动力学建模与非线性分析. 2014 年,韩研研^[13-14]在考虑几何非线性的情况下对双稳态压电悬臂梁进行了分析.

本文主要研究环境振动激励情况下双稳态屈曲梁压电发电结构的非线性动力学特性. 首先建立在双侧受均布磁场力情况下双稳态压电俘能器的动力学方程,利用多尺度法和 Galerkin 方法,分析不同外激励频率与外激励幅值下系统的非线性振动响应.

2015-03-11 收到第 1 稿,2015-04-23 收到修改稿.

* 国家自然科学基金(11272016, 11172009, 11072008),北京市自然科学基金(3122009),北京市教委科研项目,北京工业大学人才项目的资助项目
[†] 通讯作者 E-mail: caostar@bjut.edu.cn

1 双稳态压电发电结构动力学方程

双稳态屈曲梁压电发电结构如图1所示,该模型由层合屈曲梁、质量块、弹簧、以及提供均布磁场力的永磁体构成. 在环境振动条件下,质量振动驱动屈曲梁变形,层合梁中压电层由于压电效应从而产生电能.

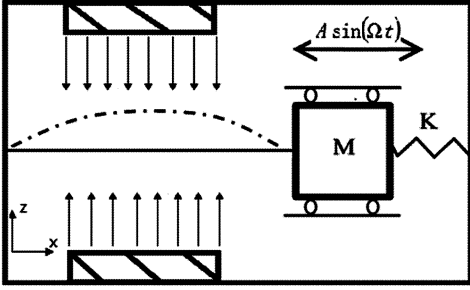


图1 双稳态屈曲梁模型

Fig.1 Model of the bistable buckled beam

根据文献[14]可获得磁场力简化形式如下,

$$F = \frac{1}{2\mu_0} B^2 S$$

式中 B 为磁场与导磁材料作用面处的磁感应强度,

$$B = \frac{B_r}{\pi} \left[\tan^{-1} \frac{LW}{2x\sqrt{L^2 + W^2 + 4x^2}} - \tan^{-1} \frac{LW}{2(x+H)\sqrt{L^2 + W^2 + 4(x+H)^2}} \right],$$

H 为磁场与导磁材料作用面处的磁场强度, S 为磁场与导磁材料作用面的面积.

进一步,基于Hamilton原理,可建立环境振动激励作用下双侧受均布磁场力作用的双稳态屈曲梁非线性运动方程.

$$\begin{aligned} & -m\ddot{w}_d - c\dot{w}_d + \frac{M}{2} \left(\frac{\partial^2}{\partial t^2} \int_0^l w_d'^2 dx \right) w_d'' + \\ & a_1 w_d'' + a_2 w_d^{(4)} + a_3 w_d'^2 + a_4 w_d' + a_5 w_d' w_d'' + \\ & a_6 w_d'' w_d'^2 + M w_d'' A \Omega^2 \sin(\Omega t) + a_7 w_d + \\ & a_8 w_d^2 = 0 \end{aligned} \quad (1)$$

其中, m 为层合梁质量, M 为质量块质量, c 为阻尼系数, w_d 为梁的横向位移, A 为外激励振幅, Ω 为外激励频率.

2 一阶离散与幅频响应分析

考虑振型函数 $w_d = W(t) \varphi_i(x)$,其中

$$\varphi_i(x) = C_i \left\{ \cosh \beta_i x - \cos \beta_i x + \right.$$

$$\left. (\sin \beta_i x - \sinh \beta_i x) \frac{\cos \beta_i l - \cosh \beta_i l}{\sin \beta_i l - \sinh \beta_i l} \right\}$$

$$1 - \cos(\beta_i l) \cosh(\beta_i l) = 0$$

$$C_i = \int_0^l \varphi_i^2 dx = 1$$

对方程(1)进行一阶 Galerkin 离散得到

$$m \ddot{W} + c \dot{W} + b_1 (\dot{W}^2 + W \ddot{W}) W + b_2 W + b_3 W^2 + b_4 W^3 = 0 \quad (2)$$

其中, $b_1 = \frac{8M\pi^4}{l^3}$,

$$b_2 = \frac{4a_1\pi^2}{l^2} - \frac{16a_2\pi^4}{l^4} + \frac{2a_4\pi}{l} - \frac{MA\Omega^2\pi^2}{l^2} \sin(\Omega t),$$

$$b_3 = \frac{4a_5\pi^3}{l^3} - \frac{4a_3\pi^2}{l^2}, \quad b_4 = \frac{16\pi^2}{l^2}.$$

引入无量纲变换

$$\bar{W} = \frac{W}{l}, \bar{A} = \frac{A}{l}, \bar{\Omega} = \frac{\Omega}{\omega_r}, \bar{t} = t\omega_r, \bar{\omega} = \frac{\omega}{\omega_r}.$$

为方便书写下面将公式中变量的上横线省略,得到系统的无量纲方程如下,

$$W + 2\xi\omega W + \omega^2 (1 - G_1 A \Omega^2 \sin \Omega t) W + G_2 W^2 + G_3 W^3 + G_4 (W \dot{W}^2 + W^2 \ddot{W}) = 0 \quad (3)$$

引入小扰动参数 ε ,

$$\xi \rightarrow \varepsilon \xi, G_1 \rightarrow \varepsilon G_1, G_2 \rightarrow \varepsilon G_2, G_3 \rightarrow \varepsilon G_3, G_4 \rightarrow \varepsilon G_4$$

得到含扰动参数的无量纲方程如下,

$$W + 2\varepsilon \xi \omega W + \omega^2 (1 - \varepsilon G_1 A \Omega^2 \sin \Omega t) W + \varepsilon G_2 W^2 + \varepsilon G_3 W^3 + \varepsilon G_4 (W \dot{W}^2 + W^2 \ddot{W}) = 0 \quad (4)$$

考虑主参数 $-1/2$ 亚谐共振,即 $\omega = \frac{\Omega}{2} + \varepsilon\sigma$,利用多尺度法对单自由度方程进行摄动分析. 设方程(4)的渐近解为

$$W = W_0(T_0, T_1) + \varepsilon W_1(T_0, T_1)$$

ε^0 阶:

$$D_0^2 W_0 + \frac{\Omega^2}{4} W_0 = 0 \quad (5)$$

ε^1 阶:

$$\begin{aligned} D_0^2 W_1 + \frac{\Omega^2}{4} W_1 = & -2D_0 D_1 W_0 - \xi \Omega D_0 W_0 + \\ & \frac{\Omega^2}{4} G_1 A \Omega^2 W_0 \sin(\Omega t) - \sigma \Omega W_0 - G_2 W_0^2 - \\ & G_3 W_0^3 - G_4 W_0 ((D_0 W_0)^2 + W_0 D_0^2 W_0) \end{aligned} \quad (6)$$

(5)式通解如下

$$W_0 = B(T_1) e^{\frac{i\Omega T_0}{2}} + \bar{B}(T_1) e^{-\frac{i\Omega T_0}{2}} \quad (7)$$

将(7)式代入(6)式右端令共振项为零,得到复数形式平均方程如下,

$$\begin{aligned}
 & -i\Omega B' - \frac{i}{2}\xi\Omega^2 B - \frac{i}{8}\Omega^2 G_1 A \Omega^2 \bar{B} - \sigma\Omega B - \\
 & 3G_3 B^2 \bar{B} + G_4 \frac{\Omega^2}{4} B^2 \bar{B} = 0 \quad (8)
 \end{aligned}$$

令 $B(T_1) = \frac{1}{2}a(T_1)e^{i\beta(T_1)}$, 将其代入(8), 并使实部虚部分别得零, 得到极坐标形式的平均方程:

$$\alpha' = -\frac{1}{2}\xi\alpha\Omega - \frac{1}{8}\Omega G_1 A \Omega^2 \alpha \cos(2\beta) \quad (9)$$

$$\beta' = \frac{1}{8}\Omega G_1 A \Omega^2 \sin(2\beta) + \sigma + \frac{3}{4\Omega} G_3 \alpha^2 - \frac{1}{16} G_4 \Omega \alpha^2 \quad (10)$$

在稳态响应情况下方程(10)式可以写成如下形式,

$$\frac{1}{8}\Omega G_1 A \Omega^2 \cos(2\beta) = -\frac{1}{2}\xi\Omega \quad (11)$$

$$\frac{1}{8}\Omega G_1 A \Omega^2 \sin(2\beta) = -\sigma - \frac{3}{4\Omega} G_3 \alpha^2 + \frac{1}{16} G_4 \Omega \alpha^2 \quad (12)$$

将方程(11),(12)两式平方相加后得到幅频响应方程,

$$16\xi^2 + \left(\frac{8\sigma}{\Omega} + \frac{6}{\Omega^2} G_3 \alpha^2 - \frac{G_4}{2} \alpha^2\right)^2 = A^2 \Omega^4 G_1^2 \quad (13)$$

根据相关实验数据和参数, 计算得到方程(13)中各项参数分别为 $\xi = 0.24$, $G_1 = 289.75$, $G_3 = 684.34$, 经数值模拟可得系统幅频响应曲线. 图2所示为改变粘性阻尼系数时系统幅频响应, 结果表明粘性阻尼抑制了响应振幅的增大, 较大的阻尼对应于较小的频响振幅.

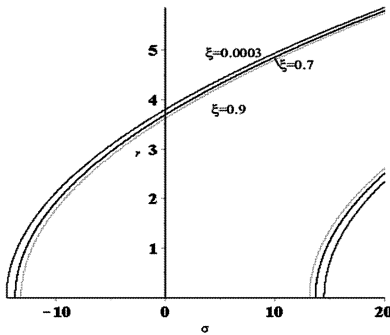


图2 不同粘滞阻尼下的幅频响应曲线

Fig.2 Amplitude-frequency curves with different viscous damping

保持其他参数不变, 改变外激励振幅, 得到系统幅频响应曲线(图3). 由此可见, 激励振幅增大会导致幅频响应振幅增大. 随着调谐参数 σ 的增

大, 频响曲线从低振幅处跳到高振幅处.

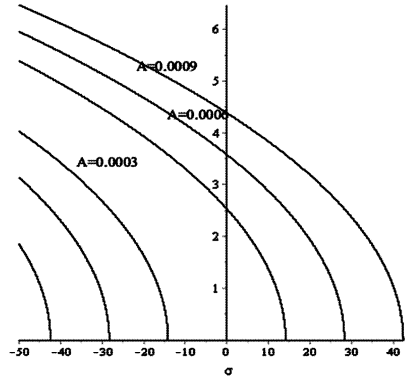


图3 不同外激励振幅下的幅频响应曲线

Fig.3 Amplitude-frequency curves under different external excited amplitudes

图4所示为外激励频率 Ω 对幅频响应曲线的影响. 激励频率 Ω 不同, 频响曲线的弯曲方向也不同. 当激励频率小于13.4的时候, 系统呈现软弹簧特性; 当激励频率增大之后, 系统开始呈现硬弹簧特性. 当激励频率变化时, 系统会出现多值现象和跳跃现象. 随着激励频率 Ω 的增大, 系统软弹簧特性的频响振幅逐渐增大, 系统硬弹簧特性的频响振幅逐渐减小.

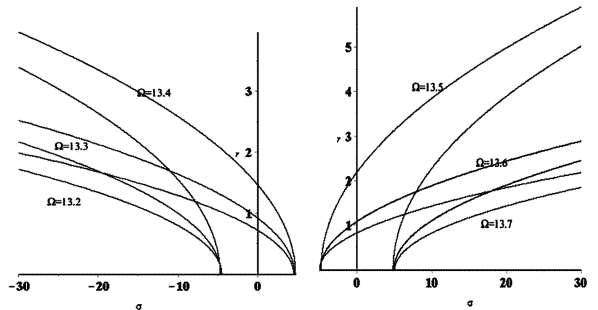


图4 不同外激励频率下的幅频响应曲线

Fig.4 Amplitude-frequency curves of different external excited frequencies

3 二阶离散与摄动分析

研究屈曲梁的二阶横向振动, 取振动模式为

$$w_d = W_1 \varphi_1 + W_2 \varphi_2 \quad (14)$$

利用 Galerkin 方法对动力学方程(1)进行离散可得,

$$\begin{aligned}
 & \ddot{W}_1 + \frac{c}{m} \dot{W}_1 + \left[\frac{Q_1}{2} (\dot{W}_1^2 + W_1 \ddot{W}_1) + \right. \\
 & \left. 2Q_1 (\dot{W}_2^2 + W_2 \ddot{W}_2) \right] W_1 +
 \end{aligned}$$

$$\begin{aligned} & \omega_1^2 \left[1 - \frac{Q_3}{Q_2} A \Omega^2 \sin(\Omega t) \right] W_1 + Q_4 W_2 + \\ & Q_5 W_1 W_2 + Q_6 W_1^2 + Q_7 W_1^2 W_2 + Q_8 W_1 W_2^2 + \\ & Q_9 W_1^3 + 2Q_{10} W_2^3 = 0 \end{aligned} \quad (15a)$$

$$\begin{aligned} & \ddot{W}_2 + \frac{c}{m} \dot{W}_2 + \left[2Q_1 (\dot{W}_1^2 + W_1 \ddot{W}_1) + \right. \\ & \left. 8Q_1 (\dot{W}_2^2 + W_2 \ddot{W}_2) \right] W + \\ & \omega_2^2 \left[1 - \frac{4Q_3}{Q_{10}} A \Omega^2 \sin(\Omega t) \right] W_2 - Q_{11} W_1 + \\ & 8Q_6 W_1 W_2 + Q_{12} W_1^2 + Q_{13} W_2^2 + Q_8 W_1^2 W_2 + \\ & Q_{14} W_1 W_2^2 + 16Q_9 W_2^3 + Q_{15} W_1^3 = 0 \end{aligned} \quad (15b)$$

引入无量纲变量

$$\bar{W}_i = \frac{W_i}{l}, \bar{A} = \frac{A}{l}, \bar{\Omega} = \frac{\Omega}{\omega_r}, \bar{t} = t\omega_r, \bar{\omega}_i = \frac{\omega_i}{\omega_r} \quad (17)$$

其中 ω_r 为无阻尼、不含压电层梁的一阶共有频率。

选取 1:2 内共振关系

$$\omega_1^2 = \Omega^2 + \varepsilon\sigma_1, \omega_2^2 = 4\Omega^2 + \varepsilon\sigma_2, 2\omega_1 \approx \omega_2 \quad (18)$$

其中 σ_1 与 σ_2 为调谐参数。引入小扰动参数 ε 同时书写方便舍去无量纲变量的上横线, 得到含扰动项的无量纲形式两自由度控制方程,

$$\begin{aligned} & \ddot{W}_1 + \varepsilon\beta_1 \dot{W}_1 + \left[\frac{\varepsilon\beta_2}{2} (\dot{W}_1^2 + \right. \\ & \left. W_1 \ddot{W}_1) + 2\varepsilon\beta_2 (\dot{W}_2^2 + W_2 \ddot{W}_2) \right] W_1 + \\ & \omega_1^2 [1 - \varepsilon\beta_3 A \Omega^2 \sin(\Omega t)] W_1 + \varepsilon\beta_4 W_2 + \\ & \varepsilon\beta_6 W_1^2 + \varepsilon\beta_7 W_1^2 W_2 + \varepsilon\beta_8 W_1 W_2^2 + \varepsilon\beta_9 W_1^3 + \\ & \varepsilon\beta_{10} W_2^3 = 0 \end{aligned} \quad (19)$$

$$\begin{aligned} & \ddot{W}_2 + \varepsilon\beta_1 \dot{W}_2 + \left[2\varepsilon\beta_2 (\dot{W}_1^2 + \right. \\ & \left. W_1 \ddot{W}_1) + 8\varepsilon\beta_2 (\dot{W}_2^2 + W_2 \ddot{W}_2) \right] W_2 + \\ & \omega_2^2 [1 - \varepsilon\beta_{10} A \Omega^2 \sin(\Omega t)] W_2 - \varepsilon\beta_{11} W_1 + \\ & \varepsilon\beta_6 W_1 W_2 + \varepsilon\beta_{12} W_1^2 + \varepsilon\beta_{13} W_2^2 + \varepsilon\beta_8 W_1^2 W_2 + \\ & \varepsilon\beta_{10} W_1 W_2^2 + \varepsilon\beta_9 W_2^3 + \varepsilon\beta_{14} W_1^3 = 0 \end{aligned} \quad (20)$$

运用多尺度方法进行摄动分析, 设方程(20)

的一致渐近解为

$$\begin{aligned} W_1 &= W_{10}(T_0, T_1) + \varepsilon W_{11}(T_0, T_1) \\ W_2 &= W_{20}(T_0, T_1) + \varepsilon W_{21}(T_0, T_1) \end{aligned} \quad (21)$$

将(21)式代入(20)式得到

ε^0 阶

$$D_0^2 W_{10} + \Omega^2 W_{10} = 0 \quad (22)$$

$$D_0^2 W_{20} + 4\Omega^2 W_{20} = 0 \quad (23)$$

ε^1 阶

$$\begin{aligned} D_0^2 W_{11} + \Omega^2 W_{11} &= -2D_0 D_1 W_{10} - \left\{ \frac{1}{2} \beta_2 [(D_0 W_{10})^2 + \right. \\ & \left. W_{10} D_0^2 W_{10}] + 2\beta_2 [(D_0 W_{20})^2 + W_{20} D_0^2 W_{20}] \right\} W_{10} + \\ & \beta_3 A \Omega^4 W_{10} \sin(\Omega t) - W_{10} \sigma_1 - \beta_4 W_{20} - \beta_5 W_{10} W_{20} - \\ & \beta_6 W_{10}^2 - \beta_7 W_{10}^2 W_{20} - \beta_8 W_{10} W_{20}^2 - \beta_9 W_{10}^3 - \beta_{10} W_{20}^3 \end{aligned} \quad (24)$$

$$\begin{aligned} D_0^2 W_{21} + 4\Omega^2 W_{21} &= -2D_0 D_1 W_{20} - \beta_1 D_0 W_{20} - \\ & \left\{ 2\beta_2 [(D_0 W_{10})^2 + W_{10} D_0^2 W_{10}] + \right. \\ & \left. 8\beta_2 [(D_0 W_{20})^2 + W_{20} D_0^2 W_{20}] \right\} W_{20} + \\ & 4\beta_{10} A \Omega^4 W_{20} \sin(\Omega t) - W_{20} \sigma_2 + \beta_{11} W_{10} - \\ & \beta_6 W_{10} W_{20} - \beta_{12} W_{10}^2 - \beta_{13} W_{20}^2 - \beta_8 W_{10}^2 W_{20} + \\ & \beta_{10} W_{10} W_{20}^2 + \beta_9 W_{20}^3 + \beta_{14} W_{10}^3 \end{aligned} \quad (25)$$

由方程(22)和(23)可得到通解如下

$$W_{10} = A_1(T_1) e^{i\Omega T_0} + \bar{A}_1(T_1) e^{-i\Omega T_0} \quad (26)$$

$$W_{20} = A_2(T_1) e^{2i\Omega T_0} + \bar{A}_2(T_1) e^{-2i\Omega T_0} \quad (27)$$

将(26)式和(27)式代入方程(24), (25), 令长期项得零得到复数形式的方程

$$\begin{aligned} 2i\Omega A_1' + \beta_1 i\Omega A_1 - \beta_2 A_1^2 \bar{A}_1 \Omega^2 + A_1 \sigma_1 + \\ \beta_3 \bar{A}_1 A_2 + 2\beta_8 A_1 A_2 \bar{A}_2 + 3\beta_9 A_1^2 \bar{A}_1 = 0 \end{aligned} \quad (28)$$

$$\begin{aligned} 4i\Omega A_2' + 2\beta_1 i\Omega A_2 - 64\beta_2 A_2^2 \bar{A}_2 \Omega^2 + A_2 \sigma_2 + \\ \beta_{12} A_1^2 + 2\beta_8 A_1 \bar{A}_1 A_2 + 48\beta_9 A_2^2 \bar{A}_2 = 0 \end{aligned} \quad (29)$$

在直角坐标系下, 令

$$A_1(T_1) = \frac{1}{2} [x_1(T_1) + ix_2(T_1)] \quad (30)$$

$$A_2(T_1) = \frac{1}{2} [x_3(T_1) + ix_4(T_1)] \quad (31)$$

将(30)和(31)式代入(28), (29)式中, 分离实部与虚部, 得到直角坐标系下的平均方程如下,

$$\begin{aligned} \dot{x}_1 &= -\frac{1}{2} \beta_1 x_1 + \frac{1}{8} \beta_2 \Omega (x_2^3 + x_1^2 x_2) - \frac{\sigma_1}{2\Omega} x_2 - \\ & \frac{\beta_5}{4\Omega} (x_1 x_4 - x_2 x_3) - \frac{\beta_8}{4\Omega} (x_2 x_3^2 + x_2 x_4^2) - \\ & \frac{3\beta_9}{8\Omega} (x_1^2 x_2 + x_2^3) \end{aligned} \quad (32)$$

$$\begin{aligned} \dot{x}_2 &= -\frac{1}{2} \beta_1 x_2 + \frac{1}{8} \beta_2 \Omega (x_1^3 + x_1^2 x_2) - \frac{\sigma_1}{2\Omega} x_1 + \\ & \frac{\beta_5}{4\Omega} (x_1 x_3 + x_2 x_4) + \frac{\beta_8}{4\Omega} (x_1 x_3^2 + x_1 x_4^2) + \\ & \frac{3\beta_9}{8\Omega} (x_2^2 x_1 + x_1^3) \end{aligned} \quad (33)$$

$$\dot{x}_3 = -\frac{1}{2}\beta_1 x_3 + 4\beta_2 \Omega (x_4^3 + x_3^2 x_4) - \frac{\sigma_2}{4\Omega} x_4 - \frac{\beta_{12}}{4\Omega} x_1 x_2 - \frac{\beta_8}{4\Omega} (x_4 x_1^2 + x_4 x_2^2) - \frac{3\beta_9}{8\Omega} (x_3^2 x_4 + x_4^3) \quad (34)$$

$$\dot{x}_4 = -\frac{1}{2}\beta_1 x_4 + 4\beta_2 \Omega (x_3^3 + x_4^2 x_3) - \frac{\sigma_2}{4\Omega} x_3 + \frac{\beta_{12}}{8\Omega} (x_1^2 - x_2^2) + \frac{\beta_8}{8\Omega} (x_3 x_1^2 + x_3 x_2^2) + \frac{3\beta_9}{8\Omega} (x_4^2 x_3 + x_3^3) \quad (35)$$

4 数值模拟

利用四阶 Runge-Kutta 法对所得到的平均方程进行模拟,通过相图和波形图可以反映系统的非线性动力学行为. 系统所选参数和初值分别为

$$\beta_1 = 1.1 \times 10^{-3}, \beta_2 = 0.04, \beta_3 = 61.37, \beta_8 = 1.7 \times 10^3, \beta_9 = 217.43, \beta_{12} = -2.6, (x_{10}, x_{20}, x_{30}, x_{40}) = (0.01, 0.02, 0.01, 0.005).$$

当改变外激励频率时,系统分别出现单倍周期,多倍周期,混沌现象. 图 5~7 分别表示外激励频率为 1.4、5.6 和 7.1 是系统的波形图和相图,系统分别产生单倍周期运动,多倍周期运动和混沌运动.

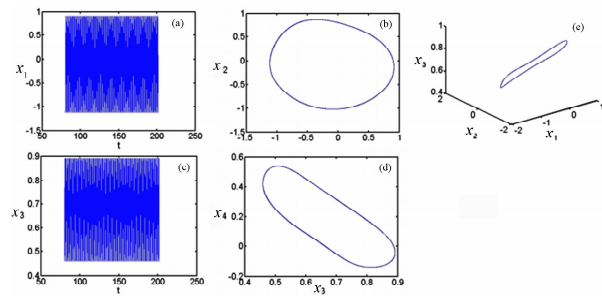


图5 单倍周期运动

Fig.5 Single periodic motion

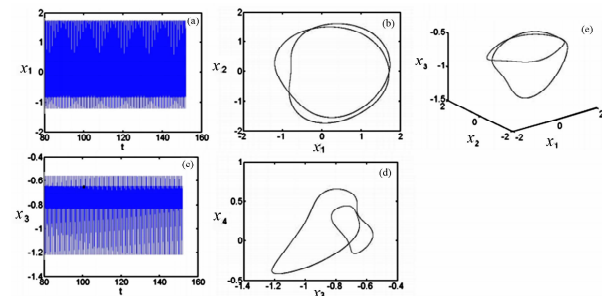


图6 多倍周期运动

Fig.6 Multiple periodic motion

现混沌现象.

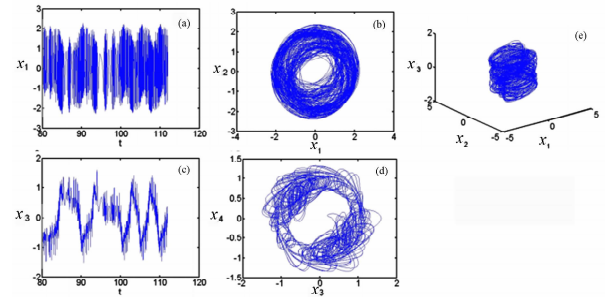


图7 混沌运动

Fig.7 Chaotic motion

5 结论

本文在考虑几何非线性的情况下,建立了固定边界条件下的双稳态屈曲梁压电俘能器的动力学控制方程. 分析了不同外激励频率与外激励幅值下该结构的振动特性,获得频率响应曲线. 发现减小系统阻尼增大外激励振幅可拓宽频率带宽. 综合应用多尺度法和 Galerkin 离散方法对系统在 1:2 内共振情况下的动力学响应进行了分析. 数值模拟后,发现在外激励作用下系统出现单倍周期,多倍周期与混沌运动.

参 考 文 献

- 季进臣,陈予恕,叶敏,张文德,郎作贵. 参激屈曲梁的倍周期分岔和混沌运动的实验研究. 实验力学, 1997, 2: 248 ~ 259 (Ji J C, Chen Y S, Ye M, Zhang W D, Lang Z G. Experimental investigation on the period doubling bifurcation and chaotic motions of a parametrically excited buckled beam. *Journal of Experimental Mechanics*, 1997, 2: 248 ~ 259 (in Chinese))
- Mattias V. An analytical analysis of a compressed bistable buckled beam. *Sensors and Actuators*, 1998, A69: 212 ~ 216
- 叶敏,陈予恕. 弹性屈曲梁在参数激励下的倍周期分叉. 固体力学学报, 1998, 19(4): 361 ~ 364 (Ye M, Chen Y S. Period doubling bifurcation in elastic buckled beam under parametric excitation. *ACTA Mechanica Sinica*, 1998, 19(4): 361 ~ 364 (in Chinese))
- Taher M, Saif A. On a tunable bistable MEMS-theory and experiment. *Journal of Microelectromechanical Systems*, 2000, 9(2): 157 ~ 170
- 赵剑,贾建援,王洪喜,张文波. 双稳态屈曲梁的非线性跳跃特性研究. 西安电子科技大学学报(自然科学版), 2007, 34(3): 458 ~ 462 (Zhao J, Jia J Y, Wang H X,

由图 7 可见,当外激励频率达到 7.1 时系统出

- Zhang W B. Nonlinear snap-through characteristic of a compressed bistable buckled beam. *Journal of Xidian University*, 2007, 34(3): 458 ~ 462 (in Chinese))
- 6 Yabuno H, Tsumoto K. Experimental investigation of a buckled beam under high-frequency excitation. *Archive of Applied Mechanics*, 2007, 77: 339 ~ 351
- 7 Cazottes P, Fernandes A, Pouget J, Hafez M. Bistable buckled beam: modeling of actuating force and experimental validations. *Journal of Mechanical Design*, 2009, 131(10)
- 8 Anton S R, Sodano H A. A review of power harvesting using piezoelectric materials (2003-006). *Smart Materials and Structures*, 2007, 16(3): 1 ~ 21
- 9 A Erturk, D J Inman. A distributed parameter electromechanical model for cantilevered piezoelectric energy harvesters. *Journal of Vibration and Acoustics*, 2008, 130(4): 041002
- 10 A Erturk, D J Inman. On mechanical modeling of cantilevered piezoelectric vibration energy harvesters. *Journal of Intelligent Material Systems and Structures*, 2008, 19(19): 1311 ~ 1325
- 11 杨增涛. 新型压电器件的机电耦合分析与结构设计[博士学位论文]. 长沙: 中南大学, 2009 (Yang Z T. Electromechanical coupling analysis and structural design on novel piezoelectric device[PhD Thesis]. Changsha: Central South University, 2009 (in Chinese))
- 12 Masana R, Daqaq M F. Electromechanical modeling and nonlinear analysis of axially loaded energy harvesters. *Journal of Vibration and Acoustics*, 2011, 133(1): 53 ~ 58
- 13 韩研研, 曹树谦, 孙舒, 郭抗抗. 考虑几何非线性时双稳态压电悬臂梁响应分析. *压电与声光*, 2014, 36(1): 132 ~ 139 (Han Y Y, Cao S Q, Sun S, Guo K K. Response analysis of bistable piezoelectric cantilever beam considering geometric nonlinearity. *Piezoelectrics & Acousto-optics*, 2014, 36(1): 132 ~ 139 (in Chinese))
- 14 郭抗抗, 曹树谦. 压电发电悬臂梁的非线性动力学建模及响应分析. *动力学与控制学报*, 2014, 12(1): 18 ~ 23 (Guo K K, Cao S Q. Nonlinear modeling and analysis of piezoelectric cantilever energy harvester. *Journal of Dynamics and Control*, 2014, 12(1): 18 ~ 23 (in Chinese))
- 15 王瑜. 永磁装置中磁场力的计算. *磁性材料及器件*, 2007, 38(5): 49 ~ 52 (Wang Y. Calculation of magnetic force of permanent magnet devices. *Journal of Magnetic Materials and Devices*, 2007, 38(5): 49 ~ 52 (in Chinese))

NONLINEAR DYNAMICS OF BISTABLE BUCKLED BEAM PIEZOELECTRIC HARVESTERS*

Cao Dongxing[†] Sun Peifeng Yao Minghui Hu WenHua Zhang Wei

(Beijing Key Laboratory of Nonlinear Vibrations and Strength of Mechanical Structures, College of Mechanical Engineering,
Beijing University of Technology, Beijing 100124, China)

Abstract In this paper, the nonlinear governing equation is firstly established for an energy harvester with bistable buckled beam. The nonlinear vibration response is studied using Galerkin method and the method of multiple scales. The frequency-response curves are depicted to examine the influence of excitation frequency and external excitation amplitude on the structural vibration characteristics. Based on energy analysis method (Hamilton's principle, Galerkin discretization, etc.), the nonlinear dynamics of the structure are investigated for the case of internal resonance with a ratio of 1 to 2. The numerical results show that periodic motions and chaotic motions occur in this structure system.

Key words bistable, buckled beam, energy harvester, nonlinear dynamics

Received 11 March 2015, revised 23 April 2015.

* The project supported by the National Natural Science Foundation of China (11272016, 11172009, 11072008), Beijing Municipal Natural Science Foundation (3122009) and Project of Beijing Municipal Commission of Education.

[†] Corresponding author E-mail: caostar@bjut.edu.cn